

# A graph-theory based fMRI analysis

Luca Barillaro<sup>1</sup>[0000-0002-7981-1521], Marianna Milano<sup>1,5</sup>[0000-0003-1561-725X],  
Maria Eugenia Caligiuri<sup>4</sup>[0000-0002-2030-5552], Jelle R.  
Dalenberg<sup>3,6</sup>[0000-0001-8580-5358], Giuseppe Agapito<sup>1,2</sup>[0000-0003-2868-7732],  
Michael Biehl<sup>7</sup>[0000-0001-5148-4568], and Mario Cannataro<sup>1</sup>[0000-0003-1502-2387]

- (1) Data Analytics Research Center, Department of Medical and Surgical Sciences, University “Magna Græcia” of Catanzaro, 88100 Catanzaro, Italy
  - (2) Department of Law, Economics and Social Sciences, University “Magna Græcia” of Catanzaro, 88100 Catanzaro, Italy
  - (3) Department of Neurology, University Medical Centre Groningen, University of Groningen, Groningen, The Netherlands
  - (4) Neuroscience Research Center, University “Magna Græcia” of Catanzaro, 88100 Catanzaro, Italy
  - (5) Department of Experimental and Clinical Medicine, University Magna Græcia of Catanzaro, 88100 Catanzaro, Italy
  - (6) Expertise Centre Movement Disorders Groningen, University Medical Center Groningen, Groningen, The Netherlands
  - (7) Bernoulli Institute for Mathematics, Computer Science and Artificial Intelligence, Computer Science Department, Intelligent Systems Group, University of Groningen, Groningen, The Netherlands
- luca.barillaro@unicz.it, m.milano@unicz.it, me.caligiuri@unicz.it,  
j.r.dalenberg@umcg.nl, agapito@unicz.it, m.biehl@rug.nl,  
cannataro@unicz.it

**Abstract.** In this study, we employed a clustering approach to analyze fMRI data from a publicly available dataset of patients with mild depression. We utilized the CONN toolbox, a widely recognized tool, to extract functional networks from the fMRI data. Subsequently, these networks were aligned using MULTIMAGNA++, a global multiple alignment software, to ensure consistency across individual datasets. The aligned data was then subjected to a clustering analysis to investigate the presence of distinct patterns. Our findings demonstrate that not only is it feasible to accurately cluster patients using this approach, but there is also potential to uncover previously unidentified subgroups among both control subjects and those affected by the disease. These results suggest new avenues for understanding the neurobiological underpinnings of mild depression and for developing targeted interventions.

**Keywords:** Functional Magnetic Resonance Imaging · Machine learning · Graph theory · Clustering · Global Network alignment.

## 1 Introduction

Functional Magnetic Resonance Imaging is an MRI modality that measures oxygenation changes in cerebral blood flow and provides a proxy for the activity of

the neurons in the brain. fMRI signal is sensitive to blood dynamic changes which drive the neuron firing. This relationship is known as the Blood Oxygenation Level Dependent (BOLD) effect [8].

fMRI data in general, are the subject of a growing interest since they may open the way to a deeper understanding of brain functioning and may lead to discovering hidden patterns in diseases[21].

To better understand brain functioning and pathology, it is very important to investigate how communication between brain areas changes across different tasks or due to disease. Such communication can be modeled as connections between nodes in the mathematical structure of a graph. Graph theory is a widely applied method in several fields of bioinformatics [11].

Machine learning approaches are often used to discover hidden information or patterns within data. A possible strategy is clustering, an unsupervised learning approach that aims to find groups in data [2]. Even on labeled data, as in our case, it can still unveil hidden information, e.g. a hidden group.

Here, we present a graph-based pipeline for clustering of fMRI data. To test our method, we used data from a publicly available dataset of patients with mild depression. We worked on these data with a popular tool, CONN toolbox [27], to extract networks which later we aligned through a global multiple alignment software, MULTIMAGNA++ [26] and then used this data to perform a clustering task.

The structure of this paper is the following: Section 2 describes all the background concepts involved in the experiments described in this paper; Section 3 illustrates the dataset and the proposed approach. Section 4 discusses the preliminary results, and finally, Section 5 concludes the paper.

## 2 Background

In this section, we aim to describe background concepts that are involved in the work presented in this paper. We first discuss our data type, functional magnetic resonance imaging, then we recall some machine learning and clustering concepts. In the latter, a quick recall of graph theory concepts and network alignment is made.

### 2.1 fMRI

Here we introduce a brief description of the functional Magnetic Resonance (fMRI) technique and its applications.

The Functional Magnetic Resonance Imaging (fMRI) is a form of the Magnetic Resonance Imaging (MRI). Whereas MRI provides information about anatomical structure, fMRI provides information about function over time. It was introduced by S. Ogawa et al in 1990 [19].

fMRI is based on the hemodynamic response [23]. When neurons in the brain are active, they consume more oxygen and cause increased regional blood flow.

By using a very strong magnetic field and radio waves, fMRI scanners can detect these changes in blood oxygenation and create detailed maps of brain activity.

fMRI methods can highlight the areas of the brain that are activated during specific tasks or cognitive processes. These active areas are represented as statistical maps known as activation maps, representing the regions of the brain that show a significant increase or decrease in neural activity.

Functional Magnetic Resonance Imaging (fMRI) can be divided into two main typologies based on the experimental design:

1. **Task-Based fMRI:** In task-based fMRI, participants are presented with specific tasks or stimuli while their brain activity is measured using fMRI[25][24]. The goal is to identify brain regions that are selectively activated during task performance and, when appropriate, compare these across groups or conditions.
2. **Resting-State fMRI:** Resting-state fMRI involves measuring spontaneous brain activity in the absence of any specific task or stimulation. Participants are instructed to relax and keep their minds at rest while fMRI scans are conducted. The analysis focuses on identifying intrinsic patterns of brain connectivity, known as resting-state networks (RSNs), which represent synchronized activity between different brain regions. By doing so, insights into the brain's intrinsic organization and potential biomarkers for neurological and psychiatric disorders are possible.

These typologies of fMRI reflect different experimental designs and data analysis approaches, each offering unique insights into the functional organization of the brain.

## 2.2 Machine learning

Machine learning is a branch of artificial intelligence that uses computers to learn from data and make predictions or decisions without explicit programming.

There is a distinction between supervised and unsupervised learning. In supervised learning, machine learning models are trained on labeled data to learn mappings between input and output. Popular tasks like classification and regression use this approach. Unsupervised learning, instead, involves extracting patterns or structures from unlabeled data.

Clustering [10] is part of the unsupervised learning methods and is a technique used to group similar data points based on certain features or characteristics. Clustering algorithms, such as k-means, hierarchical clustering, or DBSCAN, aim to partition data into distinct groups, or clusters, where data points within the same cluster share similarities while being dissimilar to those in other clusters.

## 2.3 Graph theory

Graph theory is a powerful formalism for modeling and analyzing complex systems composed of interconnected elements. The graph is the mathematical structure used to model relations between objects. It consists of vertices or nodes,

which represent the objects, and edges, which are the connections or relationships between these objects. Graph theory brings together lots of concepts and techniques, including paths, cycles, connectivity, trees, and a wide range of algorithms for analyzing and manipulating graphs.

In bioinformatics, graph theory is mainly used to represent and model biological entities and their interactions as networks [1]. Biological entities such as proteins, DNA, RNA, and metabolites can be effectively modeled as nodes, while their interactions and relationships are represented as edges in a graph [20]. Popular graph-based approaches deal, e.g, with genetic sequences, prediction of protein structures, and understanding metabolic pathways.

A graph is characterized by several topological indices, which quantify different aspects of its structure. Below are some key indices along with brief explanations:

- **Degree:** The number of edges connected to a node. This indicates the immediate number of connections that the node has with others in the graph.
- **Clustering Coefficient:** Measures how complete the neighborhood of a node is by calculating the proportion of actual connections between a node's neighbors to the total possible connections.
- **Global Efficiency:** Represents the average efficiency of parallel information transfer in the network, calculated as the average inverse of the shortest path length between each pair of nodes. This index provides insight into the node's centrality and its overall connectivity within the graph.
- **Cost:** Typically defines the ratio of existing edges to the maximum number of possible edges among nodes, reflecting the density of connections in the graph.
- **Average Path Length:** The average number of steps along the shortest paths for all possible pairs of network nodes. It offers a measure of the efficiency of information or traffic flow in the network.
- **Shortest Path:** The minimum path length between any two non-adjacent nodes, is important for understanding the most efficient route for communication between them.
- **Betweenness Centrality:** Measures the extent to which a node lies on paths between other nodes. Nodes with high betweenness may have considerable influence within a network by virtue of their control over information passing between others.

## 2.4 Network alignment

Network alignment is a technique that is used in bioinformatics and network science, to compare and align two or more biological networks. These networks can represent various biological entities and interactions, such as protein-protein interactions, metabolic pathways, or gene regulatory networks.

Network alignment aims to find the correspondence between nodes (biological entities) in different networks, identifying conserved functional modules and evolutionary relationships across species or biological conditions. The result of

a network alignment, allows researchers to discover, i.e., shared biological processes, and predict protein functions.

There are different typologies of network alignment. They can be distinguished between local and global.

Global alignment compares entire sequences and is suitable for identifying overall similarity, while local alignment focuses on identifying specific regions of similarity within sequences, making it ideal for detecting conserved functional elements amidst sequence variation.

Moreover, Pairwise or multiple alignments are possible: pairwise compare two sequences to identify regions of similarity. Multiple, instead, extends this concept to align three or more sequences simultaneously, enabling the identification of conserved regions and evolutionary relationships.

### 3 Material and methods

#### 3.1 Dataset description

The dataset comprises resting-state fMRI (rs-fMRI) data from 72 individuals, including 51 patients diagnosed with mild depression and 21 control subjects. The gender distribution within this group includes 19 males (6 controls) and 53 females (15 controls). Depression severity is classified according to the International Statistical Classification of Diseases and Related Health Problems, Tenth Revision (ICD-10), referencing Chapter V: Mental and Behavioral Disorders (codes F00-F99), specifically the section on Mood [affective] disorders (codes F30-F39). While the dataset specifies four types of depression (F32.0, F32.1, F34.1, F34.9), we aggregated these into a single class for analysis. Each scanning session in the dataset consists of 100 scans with a repetition time (TR) of 2.5 seconds [15]. The data<sup>1</sup> are publicly available through OpenNeuro [5][4] and have been preprocessed using fMRIPrep, a comprehensive tool for fMRI data preparation, with a voxel size set at 2x2x2 mm [9]. The dataset adheres to the Brain Imaging Data Structure (BIDS) format, which standardizes the organization of neuroimaging and behavioral data across studies by providing a consistent file and directory structure. This standardization facilitates data sharing and reusability, enhancing the potential for collaborative research and validation of findings.

#### 3.2 Pipeline description

We aimed to create a pipeline that can be automated for further development of this work. Since this work is composed of several steps, our resulting pipeline is heterogeneous. More specifically, we used a Matlab toolbox to perform analysis on the given dataset, some scripts for data manipulation, and finally another software to perform the clustering tasks.

<sup>1</sup> <https://openneuro.org/datasets/ds002748/versions/1.0.5>

We now describe which software is involved, while in the next subsection, we discuss our approach with technical details.

Given our dataset, the first step was to perform preprocessing and analyses to obtain a graph representation, i.e., an adjacency matrix.

Thus, to calculate resting state cross-correlations between brain regions we used the popular CONN toolbox [27] (release 21.a) running in Matlab (release 2023b)

From CONN toolbox results, we generated adjacency matrices. A single adjacency matrix contains graph parameters for all the patients, but to perform the multiple global alignments, we needed a single representation for a patient. Thus we used an R script to extract single edge lists, while later to perform clustering tasks we used a Python script to merge data for control and disease cases.

The multiple alignment phase was performed with MULTIMAGNA++ [26] due to its good performance as shown in [16]. Finally, the clustering experiments were conducted by using the popular Weka platform [12] for its friendly and easy-to-use environment. A synthetic description of the pipeline workflow is shown in Figure 1.

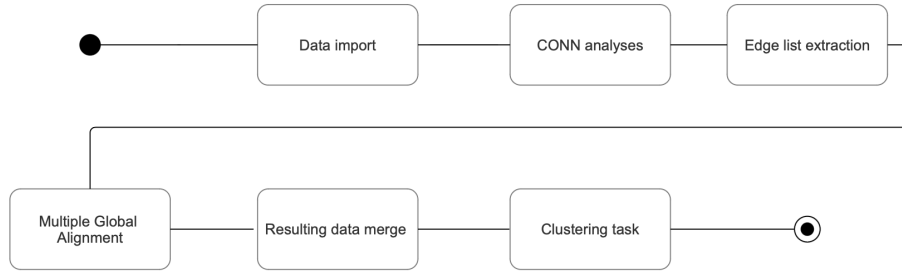


**Fig. 1.** Pipeline workflow

### 3.3 Proposed solution

As introduced earlier, given the selected dataset, we imported it into the CONN toolbox. For this purpose, we created two different projects, one for control and the other one for disease patients. Then we performed the typical analysis pipeline available in this toolbox.

After data importing through the dedicated function for the fMRIPrep pre-processed dataset, the pipeline is the following:

- **Preprocessing:** Functional data were smoothed using spatial convolution with a Gaussian kernel of 8 mm full-width half maximum (FWHM).

- **Denoising:** functional data were denoised using a standard denoising pipeline [17] including the regression of potential confounding effects characterized by white matter time-series (5 CompCor noise components), CSF time-series (5 CompCor noise components), motion parameters and their first order derivatives (12 factors) [13], outlier scans (below 62 factors) [22], session effects and their first order derivatives (2 factors), and linear trends (2 factors) within each functional run, followed by band-pass frequency filtering of the BOLD time-series[14] between  $0.008Hz$  and  $0.09Hz$ . CompCor [6][3] noise components within white matter and CSF were estimated by computing the average BOLD signal as well as the largest principal components orthogonal to the BOLD average, motion parameters, and outlier scans within each subject’s eroded segmentation masks. From the number of noise terms included in this denoising strategy, the effective degrees of freedom of the BOLD signal after denoising were estimated to range from 4.9 to 30.3 (average 26.2) across all subjects [18].
- **First-level analysis:** Seed-based connectivity maps (SBC) and ROI-to-ROI connectivity matrices (RRC) were estimated characterizing the patterns of functional connectivity with 164 HPC-ICA networks[7] and Harvard-Oxford atlas ROIs. Functional connectivity strength was calculated using Fisher-transformed bi-variate correlation coefficients from a weighted general linear model (weighted-GLM), defined separately for each pair of seed and target areas, modeling the association between their BOLD signal time-series. To compensate for possible transient magnetization effects at the beginning of each run, individual scans were weighted by a step function convolved with an SPM canonical hemodynamic response function and rectified.
- **Group-level analyses:** were performed using a General Linear Model (GLM). For each individual, voxel a separate GLM was estimated, with first-level connectivity measures at this voxel as dependent variables (one independent sample per subject and one measurement per task or experimental condition, if applicable), and groups or other subject-level identifiers as independent variables. Voxel-level hypotheses were evaluated using multivariate parametric statistics with random effects across subjects and sample covariance estimation across multiple measurements. Inferences were performed at the level of individual clusters (groups of contiguous voxels). Cluster-level inferences were based on parametric statistics from Gaussian Random Field theory [28]. Results were thresholded using a combination of a cluster-forming  $p < 0.001$  voxel-level threshold and a family-wise corrected  $p\text{-FDR} < 0.05$  cluster-size threshold[16].

Consequently, our analyses incorporate data from 164 regions of interest (ROIs). Visual representations of the networks derived from these ROIs can be viewed in Figure 2 and Figure 3.

The strength of the selected graph theory metric represents the size of the circle while edges represent the correlation values between the nodes. The shown networks represent the network of healthy and disease groups, respectively, generated using the clustering coefficient metric. By a visual analysis of these images,

it is notable that there is a different strength (bigger clustering coefficient) in the disease case group.

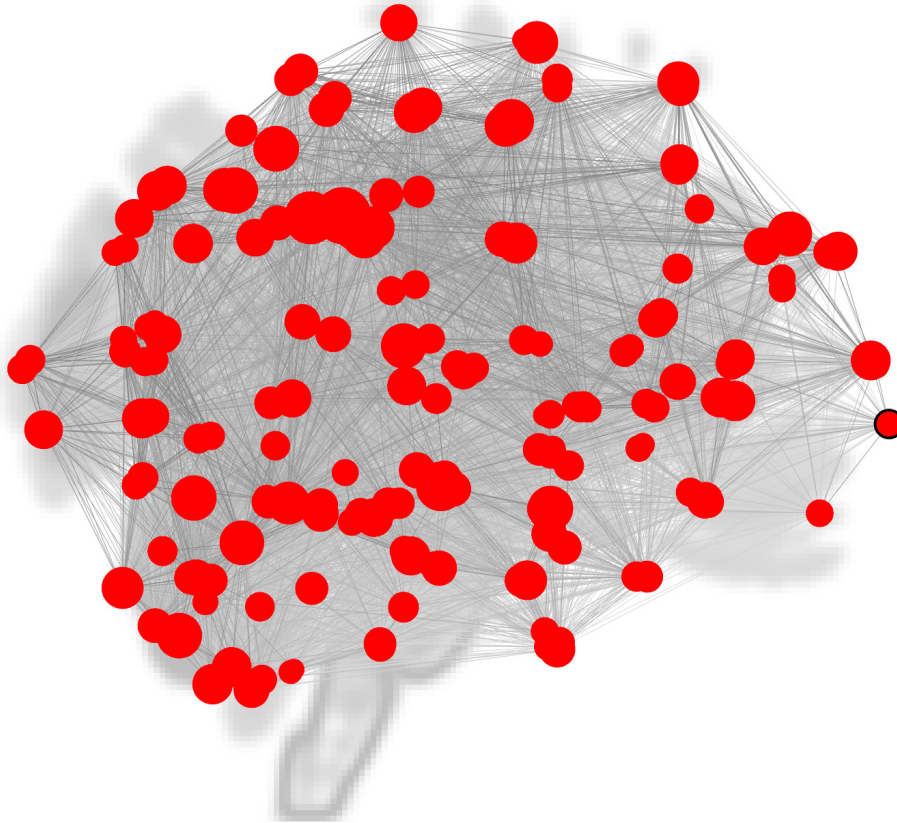


**Fig. 2.** Network of healthy control patients, generated using the clustering coefficient metric

Our interest was focused on graph theory results and, since CONN computes several graph network measures, we selected two popular graph metrics: global efficiency and clustering coefficient. As a result, from the group analysis results of ROI to ROI connectivity, we obtained a two adjacency matrix for all the patients of the given class.

To prepare data for multiple alignment steps, we extracted single edge lists for every participant from the complete adjacency matrix. We used R (version 4.3.2) and two packages: igraph (version 1.6.0) and R.matlab (version 3.7.0). We show our R script in Algorithm 1, for the control case:

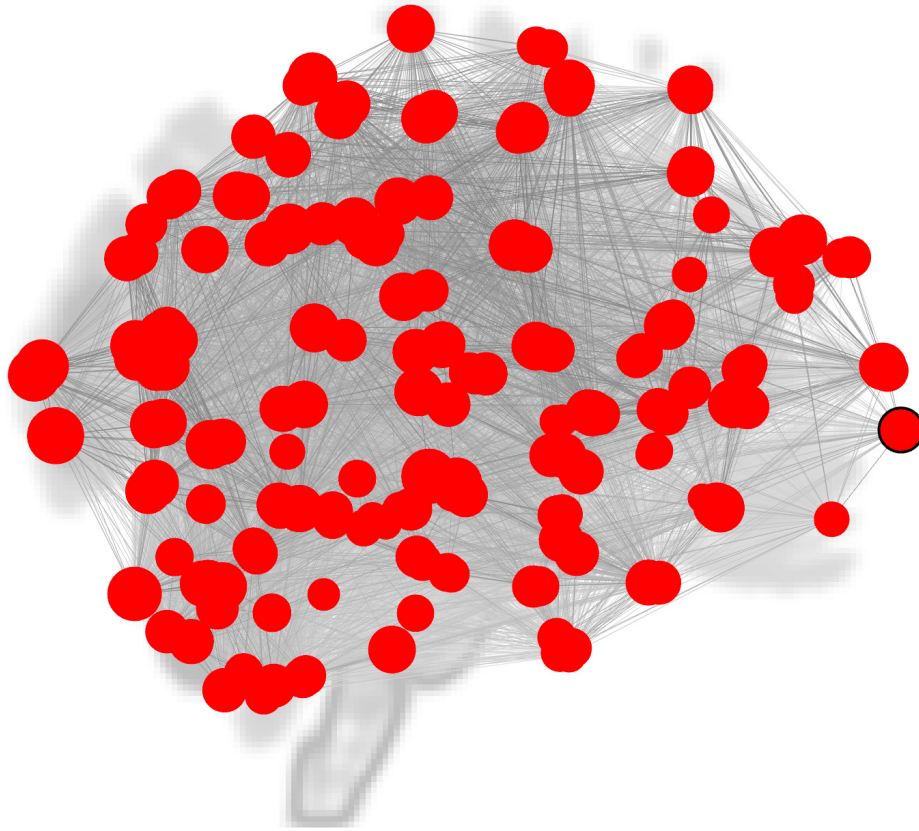


**Fig. 3.** Network of disease patients, generated using the clustering coefficient metric

---

**Algorithm 1** R script for edge list extraction

---

```

library(igraph)
library(R.matlab)
x = readMat(file.choose());
m = xA
for i = 1 : 21 do
  filename <- paste("/path/edgeListName", i, ".txt", sep = "")
  a = m[, , i]
  g = graph.adjacency(a, mode = "undirected")
  g <- simplify(g)
  list = get.edgelist(g)
  write.table(list, filename, col.names = FALSE, row.names = FALSE, sep =
"tab", quote = FALSE)
end for

```

---

We take the adjacency matrix generated by the CONN toolbox (in a Matlab data file, .mat) as input and extract a single edge list for every patient, saving them into a single text file.

Then we performed the multiple global alignment obtaining as a result single file for a patient class that is made by ROIs as rows and patient nets on columns.

Then, we manipulated data to prepare them for the clustering phase. More specifically, we merged data from alignment into a single data structure and then transposed it to have patients on rows and ROIs on columns, ending with a comma-separated value file generation. This task was performed in Python (version 3.11.7) using two packages: Pandas (version 2.1.4) and Tkinter (in tk package, version 8.6.12) We report the Python script for that task in Algorithm 2.

---

**Algorithm 2** Python script for multiple alignment merging

---

```
import pandas as pd
import tkinter as tk
from tkinter import filedialog
root = tk.Tk()
root.withdraw()
path = filedialog.askopenfilename()
df1 = pd.read_csv(path, sep='tab', header=None, engine='c')
root = tk.Tk()
root.withdraw()
path = filedialog.askopenfilename()
df2 = pd.read_csv(path, sep='tab', header=None, engine='c')
df3 = pd.concat([df1, df2], axis=1)
df4 = df3.transpose()
df4.to_csv('allTotalHTr.csv', index=False, sep='tab')
```

---

After that, we imported data into Weka (version 3.8.6) and performed several clustering tasks to check for the best results. To understand the clustering capabilities to correctly assign a patient to its group, our data are enriched with a class feature. In particular, we used it in the clustering settings, classes to clusters evaluation; using this mode, Weka first ignores the class attribute and generates the clustering. Then during the test phase, it assigns classes to the clusters, based on the majority value of the class attribute within each cluster.

We tested the clustering algorithms K-Means, Expectation Maximization, Farthest-First, and Canopy. Our interest was focused on the ability to correctly assign a patient to its group. Among all, trying different configurations, with a cluster number set to 2, K-Means resulted in better performance for our purposes, so we decided to use it for our testing. It was able to reach the lowest percentage of incorrectly clustered instances by varying the seed number, thus the clustering task was able to identify a healthy control case or a disease case.

## 4 Results

In this section, we present the results from our experiments.

As introduced earlier, we used the popular K-means method to perform clustering on global alignment data. We tested two scenarios: in the first, we evaluated the clustering ability to correctly assign a patient to its original group, so in this case our K value was set to 2.

In the second one, we tried something different, since our aim was to evaluate if a clustering with three group could find a significantly group of patient in a different stage of disease.

First we recall that the total number of patients (rows) is equal to the number of aligned networks, so we have a total of 72 rows in which the first 21 are control patients, and the remaining 51 are patients with disease.

We present our results, in a confusion matrix, for the first experiment in Table 1 and Table 2 where d stands for disease, c for control.

**Table 1.** Confusion matrix - global efficiency based network

Actual class	Predicted disease	Predicted control
Control	12	9
Disease	35	16

**Table 2.** Confusion matrix - clustering coefficient based network

Actual class	Predicted disease	Predicted control
Control	3	18
Disease	31	20

From these results we can understand that the clustering task over data from networks based on the clustering coefficient metric performs slightly better than the one with the global efficiency one. We have a total of 23 incorrectly assigned patients in the first case, and 28 in the second one.

The second experiment, with the K-means K value set to 3, is presented in a similar way to the first one, but our focus is to find if a third group is significant.

We present results for the first experiment in Table 3 and Table 4.

**Table 3.** Confusion matrix - global efficiency.

Actual class	Predicted disease	Predicted control	Third group
Control	9	7	5
Disease	21	13	17

**Table 4.** Confusion matrix - clustering coefficient.

Actual class	Predicted disease	Predicted control	Third group
Control	7	8	6
Disease	21	15	15

In this case, we can understand that the third group, takes, in both experiments, patients from the two groups, suggesting to be more investigated.

## 5 Conclusions

In conclusion, our study aimed to explore the application of machine learning techniques to graph data derived from fMRI scans. By employing a global multiple alignment method, we were able to align extracted networks and discover similarities among them. This alignment facilitated a clustering analysis, which further elucidated relationships within the data. Our methodology successfully demonstrated the capability to classify unseen data into its appropriate group based on regions of interest (ROIs) identified through multiple alignments. The results are promising and suggest that machine learning can effectively analyze fMRI graph data. However, the performance of the clustering could be enhanced by using huge data sets, and a detailed examination of preprocessing parameters to optimize the analysis.

## Acknowledgement

This work was funded by the Next Generation EU - Italian NRRP, Mission 4, Component 2, Investment 1.5, call for the creation and strengthening of 'Innovation Ecosystems', building 'Territorial R&D Leaders' (Directorial Decree n. 2021/3277) - project Tech4You - Technologies for climate change adaptation and quality of life improvement, n. ECS0000009. This work reflects only the authors' views and opinions, neither the Ministry for University and Research nor the European Commission can be considered responsible for them.

## References

1. Agapito, G., Guzzi, P.H., Cannataro, M.: Visualization of protein interaction networks: problems and solutions. *BMC bioinformatics* **14**, 1–30 (2013)
2. Agapito, G., Milano, M., Cannataro, M.: A python clustering analysis protocol of genes expression data sets. *Genes* **13**(10) (2022), <https://www.mdpi.com/2073-4425/13/10/1839>
3. Behzadi, Y., Restom, K., Liau, J., Liu, T.T.: A component based noise correction method (CompCor) for BOLD and perfusion based fMRI. *NeuroImage* **37**(1), 90–101 (Aug 2007). <https://doi.org/10.1016/j.neuroimage.2007.04.042>, <https://linkinghub.elsevier.com/retrieve/pii/S1053811907003837>

4. Bezmaternykh, D.D., Melnikov, M.Y., Savelov, A.A., Kozlova, L.I., Petrovskiy, E.D., Natarova, K.A., Shtark, M.B.: Brain Networks Connectivity in Mild to Moderate Depression: Resting State fMRI Study with Implications to Nonpharmacological Treatment. *Neural Plasticity* **2021**, 1–15 (Jan 2021). <https://doi.org/10.1155/2021/8846097>, <https://www.hindawi.com/journals/np/2021/8846097/>
5. Bezmaternykh DD, Melnikov ME, Savelov AA, Petrovskii ED: Resting state with closed eyes for patients with depression and healthy participants (2021). <https://doi.org/10.18112/OPENNEURO.DS002748.V1.0.5>, <https://openneuro.org/datasets/ds002748/versions/1.0.5>
6. Chai, X.J., Castañón, A.N., Öngür, D., Whitfield-Gabrieli, S.: Anticorrelations in resting state networks without global signal regression. *NeuroImage* **59**(2), 1420–1428 (Jan 2012). <https://doi.org/10.1016/j.neuroimage.2011.08.048>, <https://linkinghub.elsevier.com/retrieve/pii/S1053811911009657>
7. Desikan, R.S., Ségonne, F., Fischl, B., Quinn, B.T., Dickerson, B.C., Blacker, D., Buckner, R.L., Dale, A.M., Maguire, R.P., Hyman, B.T., Albert, M.S., Killiany, R.J.: An automated labeling system for subdividing the human cerebral cortex on MRI scans into gyral based regions of interest. *NeuroImage* **31**(3), 968–980 (Jul 2006). <https://doi.org/10.1016/j.neuroimage.2006.01.021>
8. DeYoe, E.A., Bandettini, P., Neitz, J., Miller, D., Winans, P.: Functional magnetic resonance imaging (fMRI) of the human brain. *Journal of Neuroscience Methods* **54**(2), 171–187 (Oct 1994). [https://doi.org/10.1016/0165-0270\(94\)90191-0](https://doi.org/10.1016/0165-0270(94)90191-0)
9. Esteban, O., Markiewicz, C.J., Blair, R.W., Moodie, C.A., Isik, A.I., Erramuzpe, A., Kent, J.D., Goncalves, M., DuPre, E., Snyder, M., Oya, H., Ghosh, S.S., Wright, J., Durnez, J., Poldrack, R.A., Gorgolewski, K.J.: fMRIPrep: a robust preprocessing pipeline for functional MRI. *Nature Methods* **16**(1), 111–116 (Jan 2019). <https://doi.org/10.1038/s41592-018-0235-4>, <https://www.nature.com/articles/s41592-018-0235-4>
10. Ezugwu, A.E., Ikotun, A.M., Oyelade, O.O., Abualigah, L., Agushaka, J.O., Eke, C.I., Akinyelu, A.A.: A comprehensive survey of clustering algorithms: State-of-the-art machine learning applications, taxonomy, challenges, and future research prospects. *Engineering Applications of Artificial Intelligence* **110**, 104743 (Apr 2022). <https://doi.org/10.1016/j.engappai.2022.104743>, <https://linkinghub.elsevier.com/retrieve/pii/S095219762200046X>
11. Farahani, F.V., Karwowski, W., Lighthall, N.R.: Application of Graph Theory for Identifying Connectivity Patterns in Human Brain Networks: A Systematic Review. *Frontiers in Neuroscience* **13** (2019), <https://www.frontiersin.org/articles/10.3389/fnins.2019.00585>
12. Frank, E., Hall, M.A., Witten, I.H.: The WEKA Workbench. Online Appendix. In: *Data Mining: Practical Machine Learning Tools and Techniques Fourth Edition*. Morgan Kaufmann (2016)
13. Friston, K.J., Williams, S., Howard, R., Frackowiak, R.S., Turner, R.: Movement-related effects in fMRI time-series. *Magnetic Resonance in Medicine* **35**(3), 346–355 (Mar 1996). <https://doi.org/10.1002/mrm.1910350312>
14. Hallquist, M.N., Hwang, K., Luna, B.: The nuisance of nuisance regression: Spectral misspecification in a common approach to resting-state fMRI preprocessing reintroduces noise and obscures functional connectivity. *NeuroImage* **82**, 208–225 (Nov 2013). <https://doi.org/10.1016/j.neuroimage.2013.05.116>, <https://linkinghub.elsevier.com/retrieve/pii/S1053811913006265>
15. ICD-10 Version:2019, <https://icd.who.int/browse10/2019/en>

16. Milano, M., Guzzi, P.H., Cannataro, M.: Network building and analysis in connectomics studies: a review of algorithms, databases and technologies. *Network Modeling Analysis in Health Informatics and Bioinformatics* **8**(1), 13 (Jun 2019). <https://doi.org/10.1007/s13721-019-0192-6>, <https://doi.org/10.1007/s13721-019-0192-6>
17. Nieto-Castanon, A.: Handbook of functional connectivity Magnetic Resonance Imaging methods in CONN. Hilbert Press (Feb 2020). <https://doi.org/10.56441/hilbertpress.2207.6598>, <https://www.hilbertpress.org/link-nieto-castanon2020>
18. Nieto-Castanon, A.: Preparing fMRI Data for Statistical Analysis (2022). <https://doi.org/10.48550/ARXIV.2210.13564>, <https://arxiv.org/abs/2210.13564>, publisher: [object Object] Version Number: 1
19. Ogawa, S., Lee, T.M., Kay, A.R., Tank, D.W.: Brain magnetic resonance imaging with contrast dependent on blood oxygenation. *Proceedings of the National Academy of Sciences of the United States of America* **87**(24), 9868–9872 (Dec 1990). <https://doi.org/10.1073/pnas.87.24.9868>
20. Pastrello, C., Otasek, D., Fortney, K., Agapito, G., Cannataro, M., Shirdel, E., Jurisica, I.: Visual data mining of biological networks: one size does not fit all. *PLoS computational biology* **9**(1), e1002833 (2013)
21. Poston, K.L., Eidelberg, D.: Functional brain networks and abnormal connectivity in the movement disorders. *NeuroImage* **62**(4), 2261–2270 (Oct 2012). <https://doi.org/10.1016/j.neuroimage.2011.12.021>, <https://www.sciencedirect.com/science/article/pii/S1053811911014236>
22. Power, J.D., Mitra, A., Laumann, T.O., Snyder, A.Z., Schlaggar, B.L., Petersen, S.E.: Methods to detect, characterize, and remove motion artifact in resting state fMRI. *NeuroImage* **84**, 320–341 (Jan 2014). <https://doi.org/10.1016/j.neuroimage.2013.08.048>, <https://linkinghub.elsevier.com/retrieve/pii/S1053811913009117>
23. Shibasaki, H.: Human brain mapping: Hemodynamic response and electrophysiology. *Clinical Neurophysiology* **119**(4), 731–743 (Apr 2008). <https://doi.org/10.1016/j.clinph.2007.10.026>, <https://www.sciencedirect.com/science/article/pii/S1388245707006578>
24. Silva, M.A., See, A.P., Essayed, W.I., Golby, A.J., Tie, Y.: Challenges and techniques for presurgical brain mapping with functional MRI. *NeuroImage. Clinical* **17**, 794–803 (2018). <https://doi.org/10.1016/j.nicl.2017.12.008>
25. Soares, J.F., Abreu, R., Lima, A.C., Sousa, L., Batista, S., Castelo-Branco, M., Duarte, J.V.: Task-based functional MRI challenges in clinical neuroscience: Choice of the best head motion correction approach in multiple sclerosis. *Frontiers in Neuroscience* **16**, 1017211 (Dec 2022). <https://doi.org/10.3389/fnins.2022.1017211>, <https://www.frontiersin.org/articles/10.3389/fnins.2022.1017211/full>
26. Vijayan, V., Milenkovic, T.: Multiple Network Alignment via MultiMAGNA+. *IEEE/ACM transactions on computational biology and bioinformatics* **15**(5), 1669–1682 (2018). <https://doi.org/10.1109/TCBB.2017.2740381>
27. Whitfield-Gabrieli, S., Nieto-Castanon, A.: Conn: a functional connectivity toolbox for correlated and anticorrelated brain networks. *Brain Connectivity* **2**(3), 125–141 (2012). <https://doi.org/10.1089/brain.2012.0073>
28. Worsley, K.J., Marrett, S., Neelin, P., Vandal, A.C., Friston, K.J., Evans, A.C.: A unified statistical approach for determining significant signals in images of cerebral activation. *Human Brain Mapping* **4**(1), 58–73 (1996). [https://doi.org/10.1002/\(SICI\)1097-0193\(1996\)4:1;58::AID-HBM4;3.0.CO;2-O](https://doi.org/10.1002/(SICI)1097-0193(1996)4:1;58::AID-HBM4;3.0.CO;2-O)